ISSN 1330–0016
CODEN FIZBE7

NEW PERSPECTIVES FOR QCD: NEAR-CONFORMAL QCD AND THE NOVEL EFFECTS OF FINAL-STATE INTERACTIONS[1]

STANLEY J. BRODSKY

Stanford Linear Accelerator Center, Stanford University, Stanford, California 94309, USA
E-mail address: sjbth@slac.stanford.edu

Received 23 October 2003; Accepted 26 April 2004
Online 16 July 2004

The effective QCD charge extracted from τ decay is remarkably constant at small momenta, implying the near-conformal behavior of hadronic interactions at small momentum transfer. The correspondence of large N_C supergravity theory in higher-dimensional anti-de Sitter spaces with gauge theory in physical space-time also has interesting implications for hadron phenomenology in the conformal limit, such as constituent counting rules for hard exclusive processes. The utility of light-front quantization and light-front Fock wavefunctions for analyzing such phenomena and representing the dynamics of QCD bound states is reviewed. The novel effects of initial- and final-state interactions in hard QCD inclusive processes, including Bjorken-scaling single-spin asymmetries and the leading-twist diffractive and shadowing contributions to deep inelastic lepton-proton scattering are also discussed.

PACS numbers: 12.38.Aw, 13.66.-a, 11.15.-q, 04.65.-e UDC 539.12.1
Keywords: hadronic interactions, deep inelastic lepton-proton scattering, supergravity theory, gauge theory, QCD, single-spin asymmetries

1. Introduction

The physical masses and inverse sizes of hadrons are characterized by the fundamental mass scale of QCD: $\Lambda_{QCD} \simeq 200$ MeV. Nevertheless, much QCD phenomenology, such as Bjorken scaling and dimensional counting rules for hard exclusive processes, can be understood from the standpoint of a theory without a fundamental scale – conformal theory.

Theoretical [1 – 4] and phenomenological [5 – 7] evidence is now accumulating that the QCD coupling becomes constant at small virtuality; i.e., $\alpha_s(Q^2)$ develops an infrared fixed point in contradiction to the usual assumption of singular growth

[1]Paper based on the talk given by S. J. Brodsky at the 2nd Int. Conference on Nuclear and Particle Physics with CEBAF at Jefferson Lab (NAPP 2003), Dubrovnik 26 – 31 May 2003. Work supported by Department of Energy contract DE-AC03-76SF00515

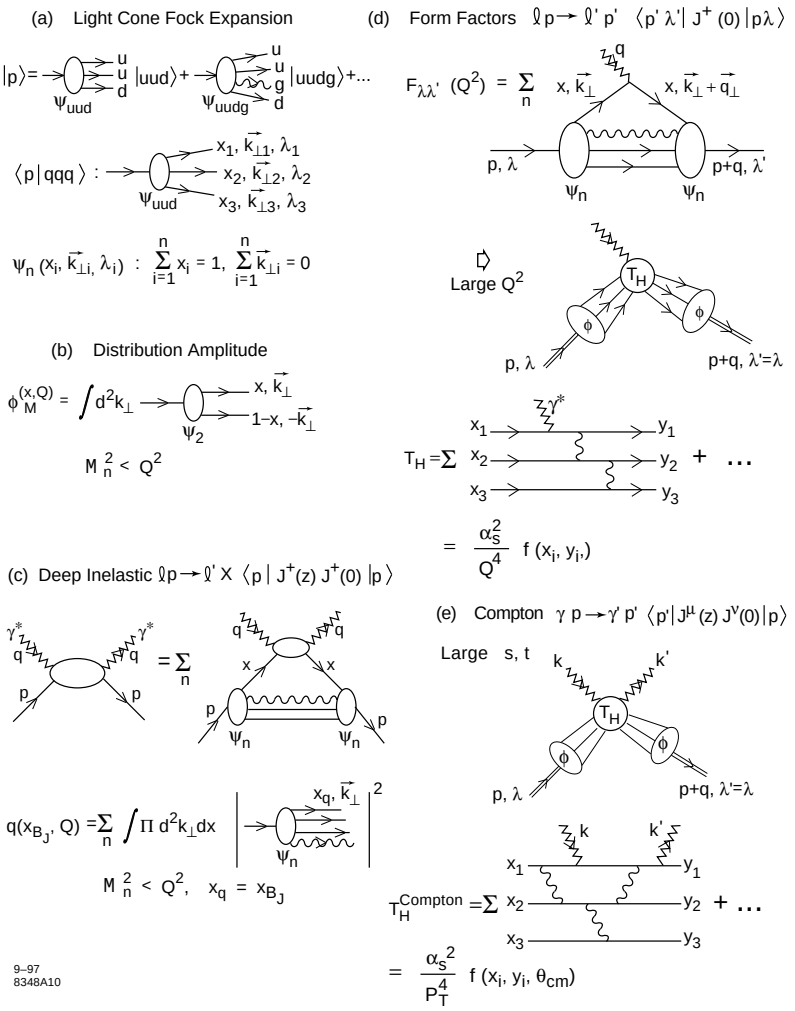

Fig. 1. Representation of QCD hadronic processes in the light-cone Fock expansion. (a) The valence uud and uudg contributions to the light-cone Fock expansion for the proton. (b) The distribution amplitude $\phi(x,Q)$ of a meson expressed as an integral over its valence light-cone wave function restricted to $q\bar{q}$ invariant mass less than Q. (c) Representation of deep inelastic scattering and the quark distributions $q(x,Q)$ as probabilistic measures of the light-cone Fock wave functions. The sum is over the Fock states with invariant mass less than Q. (d) Exact representation of spacelike form factors of the proton in the light-cone Fock basis. The sum is over all Fock components. At large momentum transfer the leading-twist contribution factorizes as the product of the hard scattering amplitude T_H for the scattering of the valence quarks collinear with the initial to final direction convoluted with the proton distribution amplitude.(e) Leading-twist factorization of the Compton amplitude at large momentum transfer.

in the infrared. If QCD running couplings are bounded, the integration over the running coupling is finite, and thus renormalon resummations are not required. If the QCD coupling becomes scale-invariant in the infrared, then elements of conformal theory become relevant even at relatively small momentum transfers.

The near-conformal behavior of QCD is the basis for commensurate scale relations [8] which relate observables to each other without renormalization scale or scheme ambiguities [9]. An important example is the generalized Crewther relation [10]. In this method the effective charges of observables are related to each other in conformal gauge theory; the effects of the nonzero QCD $\beta-$function are then taken into account using the BLM method [11] to set the scales of the respective couplings. The conformal approximation to QCD can also be used as template for QCD analyses [12, 13] such as the form of the expansion polynomials for distribution amplitudes [14].

Polchinski and Strassler [15] have derived new results for QCD in the strong coupling limit using Maldacena's string duality [16], mapping features of large N_C supergravity theory in a higher dimensional anti-de Sitter space to conformal gauge theory in 4-dimensional space-time. This correspondence has many implications for QCD in the conformal limit, allowing results usually discussed in perturbation theory, such as quark counting rules [17 – 19] and $x \to 1$ spectator counting rules [20], to be derived at all orders.

I also briefly discuss the use of the light-front Fock expansion for describing the bound-state structure of relativistic composite systems in quantum field theory. The properties of hadrons are encoded in terms of a set of frame-independent n-particle wave functions [21]. Conformal symmetry and the AdS correspondence can be used to analyze the asymptotic properties of light-front wavefunctions (LFWF), independent of perturbation theory [22]. Light-front quantization in the doubly-transverse light-cone gauge [23, 24] has a number of advantages, including explicit unitarity, a physical Fock expansion, exact representations of current matrix elements, and the decoupling properties needed to prove factorization theorems in high momentum transfer inclusive and exclusive reactions. For example, one can derive exact formulae for the weak decays of the B meson such as $B\to \ell\overline{\nu}\pi$ [25] and the deeply virtual Compton amplitude in the handbag approximation [26, 27]. Applications include two-photon exclusive reactions and diffractive dissociation into jets. The universal light-front wave functions and distribution amplitudes control hard exclusive processes such as form factors, deeply virtual Compton scattering, high momentum transfer photoproduction, and two-photon processes. The utility of light-front wave functions for the computation of various exclusive and inclusive processes is illustrated in Figs. 1 and 2.

A new understanding of the role of final-state interactions in deep inelastic scattering (DIS) has recently emerged [28]. The final-state interactions from gluon exchange between the outgoing quark and the target spectator system lead to single-spin asymmetries in semi-inclusive deep inelastic lepton-proton scattering at leading twist in perturbative QCD; i.e., the rescattering corrections of the struck quark with the target spectators are not power-law suppressed at large photon virtuality Q^2 at fixed x_{bj} [29]. The final-state interaction from gluon exchange

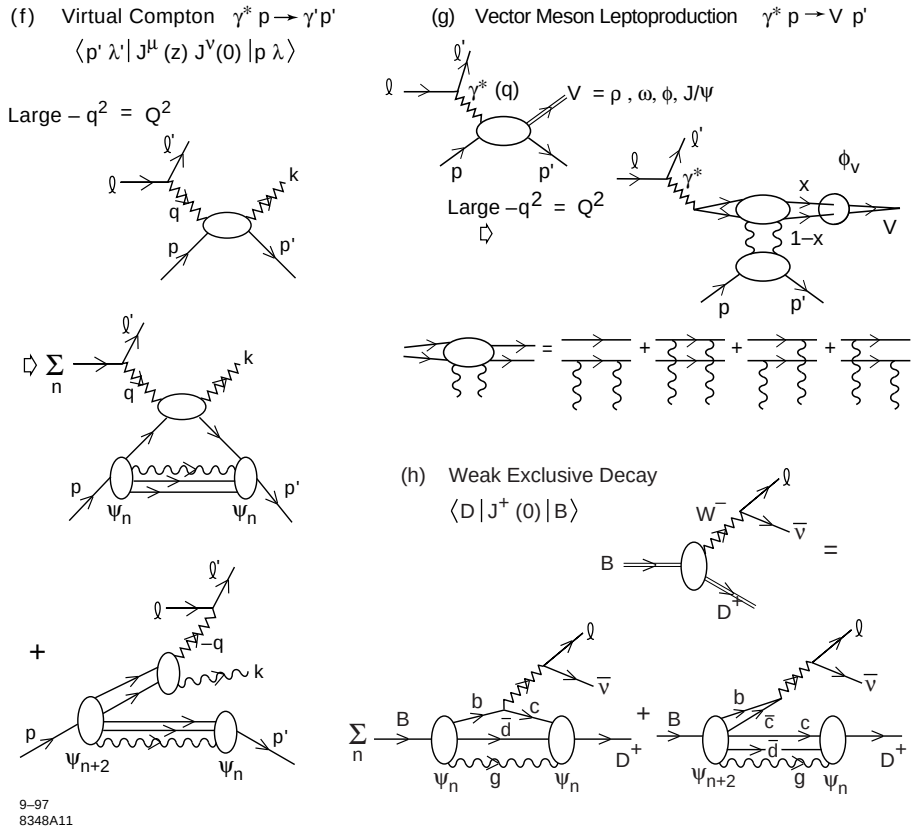

Fig. 2. (f) Representation of deeply virtual Compton scattering in the light-cone Fock expansion in the handbag approximation and at leading twist. Both diagonal $n \to n$ and off-diagonal $n+2 \to n$ contributions are required. (g) Diffractive vector meson production at large photon virtuality Q^2 and longitudinal polarization. The high energy behavior involves two gluons in the t channel coupling to the compact color dipole structure of the upper vertex. The bound-state structure of the vector meson enters through its distribution amplitude. (h) Exact representation of the weak semileptonic decays of heavy hadrons in the light-cone Fock expansion. Both diagonal $n \to n$ and off-diagonal pair annihilation $n+2 \to n$ contributions are required.

occurring immediately after the interaction of the current also produces a leading-twist diffractive component to deep inelastic scattering $\ell p \to \ell' p' X$ corresponding to color-singlet exchange with the target system; this in turn produces shadowing and anti-shadowing of the nuclear structure functions [28, 30]. In addition, one can show that the pomeron structure function derived from diffractive DIS has the same form as the quark contribution of the gluon structure function [31]. The final-state interactions occur at a light-cone time $\Delta\tau \simeq 1/\nu$ after the virtual photon interacts

with the struck quark, producing a nontrivial phase. Thus none of the above phenomena is contained in the target light-front wave functions computed in isolation. In particular, the shadowing of nuclear structure functions is due to destructive interference effects from leading-twist diffraction of the virtual photon, physics not included in the nuclear light-cone wave functions. Thus the structure functions measured in deep inelastic lepton scattering are affected by final-state rescattering, modifying their connection to light-front probability distributions. Some of these results can be understood by augmenting the light-front wave functions with a gauge link, but with a gauge potential created by an external field created by the virtual photon $q\bar{q}$ pair current [32]. The gauge link is also process dependent [33], so the resulting augmented LFWFs are not universal.

2. *The behavior of the effective QCD coupling* $\alpha_\tau(s)$

One can define the fundamental coupling of QCD from virtually any physical observable [34, 35]. Such couplings, called effective charges, are all-order resummations of perturbation theory, so they correspond to the complete theory of QCD; it is thus guaranteed that they are analytic and non-singular. For example, it has been shown that unlike the $\overline{\rm MS}$ coupling, a physical coupling is analytic across quark flavor thresholds [36, 37]. Furthermore, a physical coupling must stay finite in the infrared when the momentum scale goes to zero. In turn, this means that integrals over the running coupling are well defined for physical couplings. Once such a physical coupling $\alpha_{\rm phys}(k^2)$ is chosen, other physical quantities can be expressed as expansions in $\alpha_{\rm phys}$ by eliminating the $\overline{\rm MS}$ coupling which now becomes only an intermediary [8]. In such a procedure there are in principle no further renormalization scale (μ) or scheme ambiguities. The physical couplings satisfy the standard renormalization group equation for its logarithmic derivative, $\mathrm{d}\alpha_{\rm phys}/\mathrm{d}\ln k^2 = \widehat{\beta}_{\rm phys}[\alpha_{\rm phys}(k^2)]$, where the first two terms in the perturbative expansion of the Gell-Mann–Low function $\widehat{\beta}_{\rm phys}$ are scheme-independent at leading twist, whereas the higher order terms have to be calculated for each observable separately using perturbation theory.

In a recent paper, Menke, Merino, Rathsman and I [6] and have presented a definition of a physical coupling for QCD which has a direct relation to high precision measurements of the hadronic decay channels of the $\tau^- \to \nu_\tau \mathrm{h}^-$. Let R_τ be the ratio of the hadronic decay rate to the leptonic one. Then $R_\tau \equiv R_\tau^0\,[1 + \alpha_\tau/\pi]$, where R_τ^0 is the zeroth order QCD prediction, defines the effective charge α_τ. The data for τ decays are well-understood channel by channel, thus allowing the calculation of the hadronic decay rate and the effective charge as a function of the τ mass below the physical mass. The vector and axial-vector decay modes which can be studied separately.

Using an analysis of the tau data from the OPAL collaboration [38], we have found that the experimental value of the coupling $\alpha_\tau(s) = 0.621 \pm 0.008$ at $s = m_\tau^2$ corresponds to a value of $\alpha_{\overline{\rm MS}}(M_Z^2) = (0.117 - 0.122) \pm 0.002$, where the range corresponds to three different perturbative methods used in analyzing the data.

This result is, at least for the fixed order and renormalon resummation methods, in good agreement with the world average $\alpha_{\overline{\rm MS}}(M_Z^2) = 0.117 \pm 0.002$. However, from the figure we also see that the effective charge only reaches $\alpha_\tau(s) \sim 0.9 \pm 0.1$ at $s = 1\,\mathrm{GeV}^2$, and it even stays within the same range down to $s \sim 0.5\,\mathrm{GeV}^2$. This result is in good agreement with the estimate of Mattingly and Stevenson [5] for the effective coupling $\alpha_{\rm R}(s) \sim 0.85$ for $\sqrt{s} < 0.3\,\mathrm{GeV}$ determined from $\mathrm{e}^+\mathrm{e}^-$ annihilation, especially if one takes into account the perturbative commensurate scale relation, $\alpha_\tau(m_{\tau'}^2) = \alpha_{\rm R}(s^*)$ where, for $\alpha_{\rm R} = 0.85$, we have $s^* \simeq 0.10\, m_{\tau'}^2$. This behavior is not consistent with the coupling having a Landau pole, but rather shows that the physical coupling is close to a constant at low scales, suggesting that physical QCD couplings are effectively constant or "frozen" at low scales.

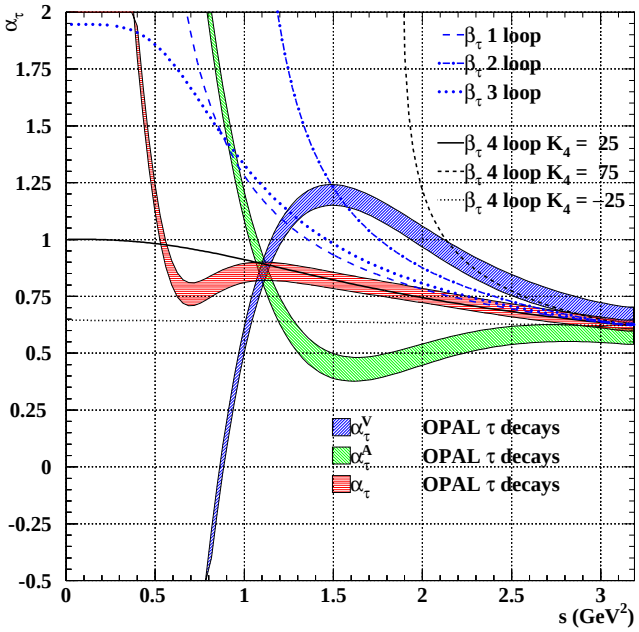

Fig. 3. The effective charge α_τ for non-strange hadronic decays of a hypothetical τ lepton with $m_{\tau'}^2 = s$ compared to solutions of the fixed order evolution equation for α_τ at two-, three-, and four-loop order. The error bands include statistical and systematic errors.

Figure 3 shows a comparison of the experimentally determined effective charge $\alpha_\tau(s)$ with solutions to the evolution equation for α_τ at two-, three-, and four-loop order normalized at m_τ. At three loops the behavior of the perturbative solution drastically changes, and instead of diverging, it freezes to a value $\alpha_\tau \simeq 2$ in the infrared. The reason for this fundamental change is the negative sign of $\beta_{\tau,2}$. This result is not perturbatively stable since the evolution of the coupling is governed by the highest order term. This is illustrated by the widely different results obtained

for three different values of the unknown four loop term $\beta_{\tau,3}$ which are also shown[2]. It is interesting to note that the central four-loop solution is in good agreement with the data all the way down to $s \simeq 1\,\mathrm{GeV}^2$.

The results for α_τ resemble the behavior of the one-loop "time-like" effective coupling [40–42]

$$\alpha_{\rm eff}(s) = \frac{4\pi}{\beta_0}\left\{\frac{1}{2} - \frac{1}{\pi}\arctan\left[\frac{1}{\pi}\ln\frac{s}{\Lambda^2}\right]\right\}, \tag{1}$$

which is finite in the infrared and freezes to the value $\alpha_{\rm eff}(s) = 4\pi/\beta_0$ as $s \to 0$. It is instructive to expand the "time-like" effective coupling for large s,

$$\begin{aligned}\alpha_{\rm eff}(s) &= \frac{4\pi}{\beta_0 \ln(s/\Lambda^2)}\left\{1 - \frac{1}{3}\frac{\pi^2}{\ln^2(s/\Lambda^2)} + \frac{1}{5}\frac{\pi^4}{\ln^4(s/\Lambda^2)} + \ldots\right\} \\ &= \alpha_{\rm s}(s)\left\{1 - \frac{\pi^2\beta_0^2}{3}\left(\frac{\alpha_{\rm s}(s)}{4\pi}\right)^2 + \frac{\pi^4\beta_0^4}{5}\left(\frac{\alpha_{\rm s}(s)}{4\pi}\right)^4 + \ldots\right\}.\end{aligned}$$

This shows that the "time-like" effective coupling is a resummation of $(\pi^2\beta_0^2\alpha_{\rm s}^2)^n$-corrections to the usual running couplings. The finite coupling $\alpha_{\rm eff}$ given in Eq. (1) obeys standard PQCD evolution at LO. Thus one can have a solution for the perturbative running of the QCD coupling which obeys asymptotic freedom but does not have a Landau singularity.

Recently it has been argued that $\alpha_{\rm R}(s)$ freezes perturbatively to all orders [3]. This should also be true perturbatively for $\alpha_\tau(s)$. In fact since all observables are related by commensurate scale relations, they all should have an IR fixed point [4]. This result is also consistent with Dyson-Schwinger equation studies of the physical gluon propagator [1, 2].

The near constancy of the effective QCD coupling at small scales helps explain the empirical success of dimensional counting rules for the power law fall-off of form factors and fixed angle scaling. As shown in Refs. [43, 44], one can calculate the hard scattering amplitude T_H for such processes [45] without scale ambiguity in terms of the effective charge α_τ or $\alpha_{\rm R}$ using commensurate scale relations. The effective coupling is evaluated in the regime where the coupling is approximately constant, in contrast to the rapidly varying behavior from powers of $\alpha_{\rm s}$ predicted by perturbation theory (the universal two-loop coupling). For example, the nucleon form factors are proportional at leading order to two powers of $\alpha_{\rm s}$ evaluated at low scales in addition to two powers of $1/q^2$; The pion photoproduction amplitude at fixed angles is proportional at leading order to three powers of the QCD coupling. The essential variation from leading-twist counting-rule behavior then only arises from the anomalous dimensions of the hadron distribution amplitudes.

[2]The values of $\beta_{\tau,3}$ used are obtained from the estimate of the four loop term in the perturbative series of R_τ, $K_4^{\overline{\rm MS}} = 25 \pm 50$ [39].

The magnitude of the effective charge $\alpha_s^{\rm exclusive}(Q^2) = F_\pi(Q^2)/4\pi Q^2 F^2_{\gamma\pi^0}(Q^2)$ for exclusive amplitudes [43] is connected to α_τ by a commensurate scale relation. Its magnitude: $\alpha_s^{\rm exclusive}(Q^2) \sim 0.8$ at small Q^2, is sufficiently large to explain the observed magnitude of exclusive amplitudes such as the pion form factor using the asymptotic distribution amplitude.

3. *Connections between QCD and conformal field theory*

As shown by Maldacena [16], there is a remarkable correspondence between large N_C supergravity theory in a higher dimensional anti-de Sitter space and supersymmetric QCD in 4-dimensional space-time. Recently, Polchinski and Strassler [15] have shown that one can use the Maldacena correspondence to compute the leading power-law falloff of exclusive processes such as high-energy fixed-angle scattering of gluonium-gluonium scattering in supersymmetric QCD. The power-law fall-off in the gauge theory reflects the warped geometry of the anti-de Sitter space in the dual theory. The resulting predictions for hadron physics coincide [15, 46, 47] with QCD dimensional counting rules [17 – 19]

$$\frac{d\sigma_{\rm H_1H_2\to H_3H_4}}{{\rm d}t} = \frac{F(t/s)}{s^{n-2}}\,, \tag{2}$$

where n is the sum of the minimal number of interpolating fields. (For a recent review of hard fixed $\theta_{\rm CM}$ angle-exclusive processes in QCD see Ref. [48].) As shown by Brower and Tan [46], the non-conformal dimensional scale which appears in the QCD analysis is set by the string constant, the slope of the primary Regge trajectory $\Lambda^2 = \alpha'_{\rm R}(0)$ of the supergravity theory. Polchinski and Strassler [15] have also derived counting rules for deep inelastic structure functions at $x \to 1$ in agreement with perturbative QCD predictions [20] as well as Bloom-Gilman exclusive-inclusive duality.

As discussed in the previous section, the QCD running coupling $\alpha_s(m_\tau^2)$ derived from hadronic τ decays is observed to be remarkably flat as a function of the τ mass, suggesting that QCD itself has an infrared fixed point and nearly conformal behavior at small virtuality.

There are other features of the superstring derivation which are of interest for QCD phenomenology:

1) The supergravity analysis is based on an extension of classical gravity theory in higher dimensions and is nonperturbative. Thus the usual analyses of exclusive processes, which were derived in perturbation theory can be extended by the Maldacena correspondence to all orders. An interesting point is that the hard scattering amplitudes which are normally of order α_s^p in PQCD, appear as order $\alpha_s^{p/2}$ in the supergravity predictions. This can be understood as an all-orders resummation of the effective potential [16, 49].

2) The superstring theory results are derived in the limit of a large N_C [50]. For gluon-gluon scattering, the amplitude scales as $1/N_C^2$. Frampton has shown how to extend the analysis to the fundamental representation [51]. For color-singlet bound states of quarks, the amplitude scales as $1/N_C$. This large N_C-counting in fact corresponds to the quark interchange mechanism [52]. For example, for $K^+p \to K^+p$ scattering, the u-quark exchange amplitude scales approximately as $(1/u)\,(1/t^2)$, which agrees remarkably well with the measured large θ_{CM} dependence of the K^+p differential cross section [53]. This implies that the nonsinglet Reggeon trajectory asymptotes to a negative integer [54], in this case, $\lim_{-t\to\infty} \alpha_R(t) \to -1$.

3) Pinch contributions corresponding to the independent scattering mechanism of Landshoff [55] are absent in the superstring derivation. This can be understood by the fact that amplitudes based on gluon exchange between color-singlet hadrons are suppressed at large N_C [22]. Furthermore, the independent scattering amplitudes are suppressed by Sudakov form factors which fall faster than any power in a theory with a fixed-point coupling such as conformal QCD [19, 56].

4) The leading-twist results for hard exclusive processes correspond to the suppression of hadron wave functions with non-zero orbital angular momentum, which is the principle underlying the selection rules corresponding to hadron helicity conservation [57]. The suppression can be understood as follows: the LF wave function with nonzero angular momentum in the constituent rest frame $\sum \boldsymbol{k}_i = 0$ can be determined by iterating the one gluon exchange kernel. They then have the structure [58, 59]

$$\psi_{L_z=1} = \frac{\boldsymbol{S}\cdot\widehat{n}\times\boldsymbol{k}_\perp}{D(k_\perp^2,x)}\psi_{L_z=0} \tag{3}$$

or

$$\psi_{L_z=1} = \frac{\widehat{\epsilon}\cdot\widehat{n}\times\boldsymbol{k}_\perp}{D(k_\perp^2,x)}\psi_{L_z=0}\,, \tag{4}$$

where the light-front energy denominator $D(k_\perp^2,x) \sim k_\perp^2$ at high transverse momentum, $\widehat{n}$ is the light-front quantization direction, and $\widehat{\epsilon}$ is a spin-one polarization vector. This leads to the Λ/Q suppression of spin-flip amplitudes in QCD. For example, such wave functions lead to the large momentum transfer prediction $A_{LL} \sim 1/3$ for $pp \to pp$ elastic scattering [22] at large angles and momentum transfer and the asymptotic prediction $F_2(t)/F_1(t) \propto t^{-2}$ modulo powers of $\log t$ [60].

4. Light-front wave functions and angular momentum

The concept of a wave function of a hadron as a composite of relativistic quarks and gluons is naturally formulated in terms of the light-front Fock expansion at

fixed light-front time, $\tau = x{\cdot}\omega$. The four-vector ω, with $\omega^2 = 0$, determines the orientation of the light-front plane; the freedom to choose ω provides an explicitly covariant formulation of light-front quantization [61]. The light-front wave functions (LFWFs) $\psi_n(x_i, k_{\perp_i}, \lambda_i)$, with $x_i = (k_i{\cdot}\omega)/(P{\cdot}\omega)$, $\sum_{i=1}^n x_i = 1$, $\sum_{i=1}^n k_{\perp_i} = 0_\perp$, are the coefficient functions for n partons in the Fock expansion, providing a general frame-independent representation of the hadron state. Matrix elements of local operators, such as spacelike proton form factors, can be computed simply from the overlap integrals of light front wave functions in analogy to nonrelativistic Schrödinger theory. In principle, one can solve for the LFWFs directly from the fundamental theory using methods such as discretized light-front quantization, the transverse lattice, lattice gauge theory moments, or Bethe–Salpeter techniques. The determination of the hadron LFWFs from phenomenological constraints and from QCD itself is a central goal of hadron and nuclear physics. Reviews of nonperturbative light-front methods may be found in Refs. [21], [61] and [62].

One of the central issues in the analysis of fundamental hadron structure is the presence of non-zero orbital angular momentum in the bound-state wave functions. The evidence for a "spin crisis" in the Ellis-Jaffe sum rule signals a significant orbital contribution in the proton wave function [63, 64]. The Pauli form factor of nucleons is computed from the overlap of LFWFs differing by one unit of orbital angular momentum $\Delta L_z = \pm 1$. Thus the fact that the anomalous moment of the proton is non-zero requires nonzero orbital angular momentum in the proton wavefunction [65]. In the light-front method, orbital angular momentum is treated explicitly; it includes the orbital contributions induced by relativistic effects, such as the spin-orbit effects normally associated with the conventional Dirac spinors.

A number of new non-perturbative methods for determining light-front wave functions have been developed including discretized light-cone quantization using Pauli-Villars regularization, supersymmetry, and the transverse lattice. One can also project the known solutions of the Bethe-Salpeter equation to equal light-front time, thus producing hadronic light-front Fock wave functions. A potentially important method is to construct the $q\overline{q}$ Green's function using light-front Hamiltonian theory, with DLCQ boundary conditions and Lippmann-Schwinger resummation. The zeros of the resulting resolvent projected on states of specific angular momentum J_z can then generate the meson spectrum and their light-front Fock wavefunctions. For a recent review of light-front methods and references, see Ref. [66].

Diffractive multi-jet production in heavy nuclei provides a novel way to measure the shape of light-front Fock state wave functions and test color transparency [67]. For example, consider the reaction [68, 69] $\pi \mathrm{A} \to \mathrm{Jet}_1 + \mathrm{Jet}_2 + \mathrm{A}'$ at high energy where the nucleus A' is left intact in its ground state. The transverse momenta of the jets balance so that $\boldsymbol{k}_{\perp i} + \boldsymbol{k}_{\perp 2} = \boldsymbol{q}_\perp < R_A^{-1}$. The light-cone longitudinal momentum fractions also need to add to $x_1 + x_2 \sim 1$ so that $\Delta p_L < R_A^{-1}$. The process can then occur coherently in the nucleus. Because of color transparency, the valence wave function of the pion with small impact separation will penetrate the nucleus with minimal interactions, diffracting into jet pairs [68]. The $x_1 = x$, $x_2 = 1 - x$ dependence of the di-jet distributions will thus reflect the shape of the pion valence light-cone wave function in x; similarly, the $\boldsymbol{k}_{\perp 1} - \boldsymbol{k}_{\perp 2}$ relative transverse

momenta of the jets gives key information on the derivative of the underlying shape of the valence pion wavefunction [69, 70]. The diffractive nuclear amplitude extrapolated to $t = 0$ should be linear in nuclear number A if color transparency is correct. The integrated diffractive rate should then scale as $A^2/R_A^2 \sim A^{4/3}$ as verified by E791 for 500 GeV incident pions on nuclear targets [71]. The measured momentum fraction distribution of the jets [72] is consistent with the shape of the pion asymptotic distribution amplitude, $\phi_\pi^{\rm asympt}(x) = \sqrt{3} f_\pi x(1-x)$. Data from CLEO [73] for the $\gamma\gamma^* \to \pi^0$ transition form factor also favor a form for the pion distribution amplitude close to the asymptotic solution to its perturbative QCD evolution equation [74, 75, 45].

In a recent work, Dae Sung Hwang, John Hiller, Volodya Karmanov and Brodsky [59] have studied the analytic structure of LFWFs using the explicitly Lorentz-invariant formulation of the front form. Eigensolutions of the Bethe-Salpeter equation have specific angular momentum as specified by the Pauli-Lubanski vector. The corresponding LFWF for an n-particle Fock state evaluated at equal light-front time $\tau = \omega \cdot x$ can be obtained by integrating the Bethe-Salpeter solutions over the corresponding relative light-front energies. The resulting LFWFs $\psi_n^I(x_i, k_{\perp i})$ are functions of the light-cone momentum fractions $x_i = (k_i \cdot \omega)/(p \cdot \omega)$ and the invariant mass squared of the constituents $M_0^2 = (\sum_{i=1}^n k_i^\mu)^2 = \sum_{i=1}^n \left[(k_\perp^2 + m^2)/x\right]_i$ and the light-cone momentum fractions $x_i = (k_i \cdot \omega)/(p \cdot \omega)$ each multiplying spin-vector and polarization tensor invariants which can involve ω^μ. The resulting LFWFs for bound states are eigenstates of the Karmanov–Smirnov kinematic angular momentum operator [76]. Thus LFWFs satisfy all Lorentz symmetries of the front form, including boost invariance, and they are proper eigenstates of angular momentum. Although LFWFs depend on the choice of the light-front quantization direction, all observables, such as matrix elements of local current operators, form factors, and cross sections, are light-front invariants – they must be independent of ω_μ.

The dependence of the LFWFs on the square of the invariant mass implies that hadron form factors computed from the overlap integrals of LFWFS are analytic functions of Q^2. In particular, the general form of the LFWFs for baryons in QCD leads to a ratio of form factors $F_2(Q^2)/F_1(Q^2)$ which behaves asymptotically as an inverse power of Q^2 modulo logarithms, in agreement with the PQCD analysis of Belitsky, Ji, and Yuan [60], as well as with form factor ratios obtained using the nonperturbative solutions to the Wick–Cutkosky model found by Karmanov and Smirnov [76]. The detailed analysis of baryon form factors at large Q^2 based on perturbative QCD predicts the asymptotic behavior $Q^2 F_2(Q^2)/F_1(Q^2) \sim \log^{2+8/(9\beta)}(Q^2/\Lambda^2)$, where $\beta = 11 - 2n_f/3$ [60]. This asymptotic logarithmic form can be generalized to include the correct $Q^2 = 0$ limit and the cut at the two-pion threshold in the timelike region. Such a parametrization is

$$F_2/F_1 = \kappa_p \frac{1 + (Q^2/C_1)^2 \log^{b+2}(1 + Q^2/4m_\pi^2)}{1 + (Q^2/C_2)^3 \log^b(1 + Q^2/4m_\pi^2)}, \tag{5}$$

where for simplicity we have ignored the small factor $8/9\beta$, as in Ref. [60]. For the

large-Q^2 region of the available data, this already reduces to the asymptotic form

$$F_2/F_1 = \kappa_p \frac{C_2^3}{C_1^2} \frac{\log^2(Q^2/4m_\pi^2)}{Q^2}. \tag{6}$$

The values of C_1, C_2 and b are not tightly constrained, except for the combination C_2^3/C_1^2. A fit to the JLab data yields $C_1 = 0.791$ GeV^2, $C_2 = 0.380$ GeV^2, and $b = 5.102$. Thus, as shown in Fig. 4, one can fit the form factor ratio over the entire measured range with an analytic form compatible with the predicted perturbative QCD asymptotic behavior. The form for spacelike form factors can be analytically continued to the time-like regime; in particular, one can test the predicted relative phase of the proton time-like form factors by measuring the single-spin asymmetry of the produced proton polarization normal to its production plane in $e^+e^- \to p\overline{p}$ [80].

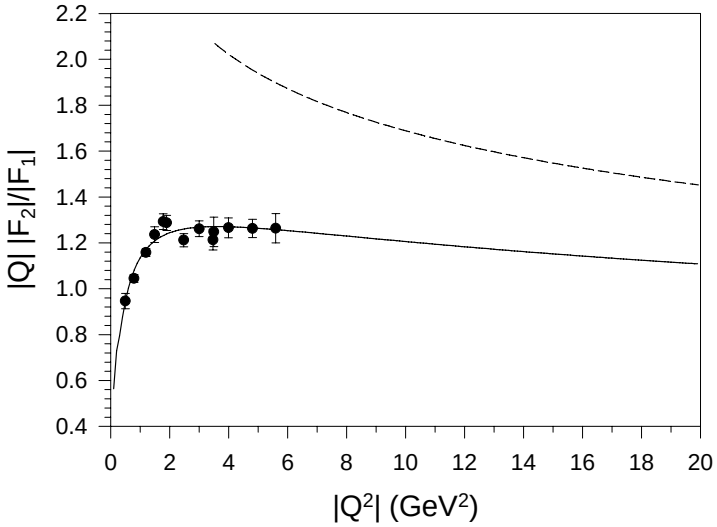

Fig. 4. Perturbative QCD motivated fit to the Jefferson Lab polarization transfer data [77, 78]. The parametrization is given in Eq. (5) of the text. The dashed line shows the predicted form for timelike $q^2 = -Q^2$. For a discussion on the validity of continuing spacelike form factors to the timelike region, see [79]

Recent advances in the calculation of hard exclusive amplitude at higher order are discussed by Duplancic and Nizic in Ref. [81] Hadronic exclusive processes are closely related to exclusive hadronic B decays, processes which are essential for determining the CKM phases and the physics of CP violation [82 – 85], such as $B \to K\pi$, $B \to \ell\nu\pi$, and $B \to Kp\overline{p}$ [86]. Recently Fred Goldhaber, Jungil Lee and Brodsky [87] have shown how one can compute the exclusive production of a glueball in association with a charmonium state in e^+e^- annihilation. Since the subprocesses $\gamma^* \to (c\overline{c})(c\overline{c})$ and $\gamma^* \to (c\overline{c})(gg)$ are of the same nominal order in perturbative QCD, it is possible that some portion of the anomalously large signal

observed by Belle [88] in $e^+e^- \to J/\psi X$ may actually be due to the production of charmonium-glueball $J/\psi \mathcal{G}_J$ pairs.

5. *Effects of final-state interactions in QCD*

Ever since the earliest days of the parton model, it has been assumed that the leading-twist structure functions $F_i(x, Q^2)$ measured in deep inelastic lepton scattering are determined by the *probability* distributions of quarks and gluons as determined by the light-cone (LC) wave functions of the target. For example, the quark distribution is

$$P_{q/N}(x_B, Q^2) = \sum_n \int^{k_{iT}^2 < Q^2} \left[\prod_i dx_i \, d^2k_{Ti}\right] |\psi_n(x_i, k_{Ti})|^2 \sum_{j=q} \delta(x_B - x_j). \qquad (7)$$

The identification of structure functions with the square of light-cone wave functions is usually made in the LC gauge, $n \cdot A = A^+ = 0$, where the path-ordered exponential in the operator product for the forward virtual Compton amplitude apparently reduces to unity. Thus the deep inelastic lepton scattering cross section appears to be fully determined by the probability distribution of partons in the target. However, Paul Hoyer, Nils Marchal, Stephane Peigne, Francesco Sannino, and Brodsky [28] have shown that the leading-twist contribution to DIS is affected by diffractive rescattering of a quark in the target, a coherent effect which is not included in the light-cone wave functions, even in light-cone gauge [28, 32, 89]. The distinction between structure functions and parton probabilities is already implied by the Glauber-Gribov picture of nuclear shadowing [90 – 94]. In this framework shadowing arises from interference between complex rescattering amplitudes involving on-shell intermediate states, as in Fig. 5. In contrast, the wave function of

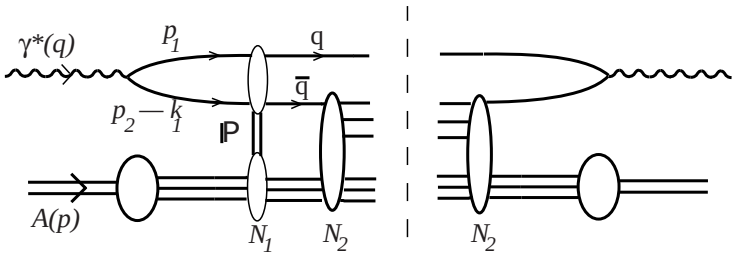

Fig. 5. Glauber-Gribov shadowing involves interference between rescattering amplitudes. .

a stable target is strictly real since it does not have on energy-shell configurations. A probabilistic interpretation of the DIS cross section is thus precluded.

It is well-known that in the Feynman and other covariant gauges one has to evaluate the corrections to the "handbag" diagram due to the final-state interactions of

the struck quark (the line carrying momentum p_1 in Fig. 6) with the gauge field of the target. In light-cone gauge, this effect also involves rescattering of a spectator quark, the p_2 line in Fig. 6. The light-cone gauge is singular – in particular, the gluon propagator

$$d^{\mu\nu}_{LC}(k) = \frac{\mathrm{i}}{\mathrm{k}^2 + \mathrm{i}\varepsilon}\left[-g^{\mu\nu} + \frac{n^\mu k^\nu + k^\mu n^\nu}{n\cdot k}\right] \tag{8}$$

has a pole at $k^+ = 0$ which requires an analytic prescription. In final-state scattering involving on-shell intermediate states, the exchanged momentum k^+ is of $O(1/\nu)$ in the target rest frame, which enhances the second term in the propagator. This enhancement allows rescattering to contribute at leading twist even in LC gauge.

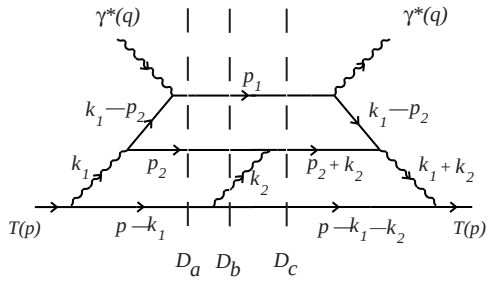

(a)

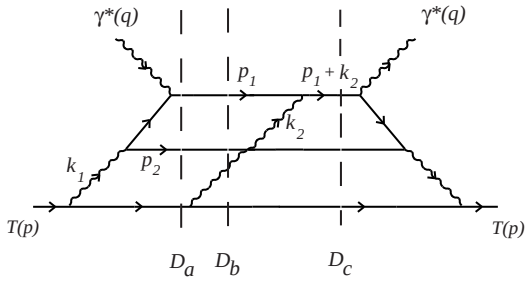

(b)

Fig. 6. Two types of final state interactions. (a) Scattering of the antiquark (p_2 line), which in the aligned jet kinematics is part of the target dynamics. (b) Scattering of the current quark (p_1 line). For each LC time-ordered diagram, the potentially on-shell intermediate states—corresponding to the zeroes of the denominators D_a, D_b, D_c—are denoted by dashed lines.

The issues involving final-state interactions even occur in the simple framework of Abelian gauge theory with scalar quarks. Consider a frame with $q^+ < 0$. We can then distinguish FSI from ISI using LC time-ordered perturbation theory, LCPTH [45]. Figure 6 illustrates two LCPTH diagrams which contribute to the forward $\gamma^*\mathrm{T} \to \gamma^*\mathrm{T}$ amplitude, where the target T is taken to be a single quark. In the aligned jet kinematics, the virtual photon fluctuates into a $\mathrm{q\overline{q}}$ pair with limited

transverse momentum, and the (struck) quark takes nearly all the longitudinal momentum of the photon. The initial q and $\overline{\mathrm{q}}$ momenta are denoted p_1 and $p_2 - k_1$, respectively.

The calculation of the rescattering effects on DIS in Feynman and light-cone gauge through three loops is given in detail in Ref. [28]. The result can be resummed and is most easily expressed in eikonal form in terms of transverse distances $r_{\mathrm{T}}, R_{\mathrm{T}}$ conjugate to $p_{2\mathrm{T}}, k_{\mathrm{T}}$. The DIS cross section can be expressed as

$$Q^4 \frac{\mathrm{d}\sigma}{\mathrm{d}Q^2\,\mathrm{d}x_{\mathrm{B}}} = \frac{\alpha_{\mathrm{em}}}{16\pi^2}\frac{1-y}{y^2}\frac{1}{2M\nu}\int \frac{\mathrm{d}p_2^-}{p_2^-}\,\mathrm{d}^2\boldsymbol{r}_{\mathrm{T}}\,\mathrm{d}^2\boldsymbol{R}_{\mathrm{T}}\,|\tilde{M}|^2 \tag{9}$$

where

$$|\tilde{M}(p_2^-, \boldsymbol{r}_{\mathrm{T}}, \boldsymbol{R}_{\mathrm{T}})| = \left|\frac{\sin\left[g^2\,W(\boldsymbol{r}_{\mathrm{T}}, \boldsymbol{R}_{\mathrm{T}})/2\right]}{g^2\,W(\boldsymbol{r}_{\mathrm{T}}, \boldsymbol{R}_{\mathrm{T}})/2}\tilde{A}(p_2^-, \boldsymbol{r}_{\mathrm{T}}, \boldsymbol{R}_{\mathrm{T}})\right| \tag{10}$$

is the resummed result. The Born amplitude is

$$\tilde{A}(p_2^-, \boldsymbol{r}_{\mathrm{T}}, \boldsymbol{R}_{\mathrm{T}}) = 2eg^2 MQp_2^-\,V(m_{||}r_{\mathrm{T}})W(\boldsymbol{r}_{\mathrm{T}}, \boldsymbol{R}_{\mathrm{T}}) \tag{11}$$

where $m_{||}^2 = p_2^- M x_{\mathrm{B}} + m^2$ and

$$V(m\,r_{\mathrm{T}}) \equiv \int \frac{\mathrm{d}^2\boldsymbol{p}_{\mathrm{T}}}{(2\pi)^2}\frac{e^{\mathrm{i}\boldsymbol{r}_{\mathrm{T}}\cdot\boldsymbol{p}_{\mathrm{T}}}}{p_{\mathrm{T}}^2 + m^2} = \frac{1}{2\pi}K_0(m\,r_{\mathrm{T}}). \tag{12}$$

The rescattering effect of the dipole of the $\mathrm{q}\overline{\mathrm{q}}$ is controlled by

$$W(\boldsymbol{r}_{\mathrm{T}}, \boldsymbol{R}_{\mathrm{T}}) \equiv \int \frac{\mathrm{d}^2\boldsymbol{k}_{\mathrm{T}}}{(2\pi)^2}\frac{1 - e^{\mathrm{i}\boldsymbol{r}_{\mathrm{T}}\cdot\boldsymbol{k}_{\mathrm{T}}}}{k_{\mathrm{T}}^2}e^{\mathrm{i}\boldsymbol{R}_{\mathrm{T}}\cdot\boldsymbol{k}_{\mathrm{T}}} = \frac{1}{2\pi}\log\left(\frac{|\boldsymbol{R}_{\mathrm{T}} + \boldsymbol{r}_{\mathrm{T}}|}{R_{\mathrm{T}}}\right). \tag{13}$$

The fact that the coefficient of $\tilde{A}$ in Eq. (10) is less than unity for all $\boldsymbol{r}_{\mathrm{T}}, \boldsymbol{R}_{\mathrm{T}}$ shows that the rescattering corrections reduce the cross section. It is the analog of nuclear shadowing in our model.

We have also found the same result for the DIS cross sections in light-cone gauge. Three prescriptions for defining the propagator pole at $k^+ = 0$ have been used in the literature:

$$\frac{1}{k_i^+} \to \left[\frac{1}{k_i^+}\right]_{\eta_i} = \begin{cases} k_i^+\left[(k_i^+ - \mathrm{i}\eta_i)(k_i^+ + \mathrm{i}\eta_i)\right]^{-1} & \text{(PV)} \\ \left[k_i^+ - \mathrm{i}\eta_i\right]^{-1} & \text{(K)} \\ \left[k_i^+ - \mathrm{i}\eta_i\epsilon(k_i^-)\right]^{-1} & \text{(ML)} \end{cases} \tag{14}$$

the principal-value (PV), Kovchegov (K) [95], and Mandelstam-Leibbrandt (ML) [96] prescriptions. The 'sign function' is denoted $\epsilon(x) = \Theta(x) - \Theta(-x)$. With the PV prescription we have $I_\eta = \int \mathrm{d}k_2^+\left[k_2^+\right]_{\eta_2}^{-1} = 0$. Since an individual diagram

may contain pole terms $\sim 1/k_i^+$, its value can depend on the prescription used for light-cone gauge. However, the $k_i^+ = 0$ poles cancel when all diagrams are added. The net is thus prescription-independent and agrees with the Feynman gauge result. It is interesting to note that the diagrams involving rescattering of the struck quark p_1 do not contribute to the leading-twist structure functions if we use the Kovchegov prescription to define the light-cone gauge. In other prescriptions for light-cone gauge the rescattering of the struck quark line p_1 leads to an infrared divergent phase factor $\exp(\mathrm{i}\phi)$, where

$$\phi = g^2 \, \frac{I_\eta - 1}{4\pi} \, K_0(\lambda R_T) + O(g^6) \tag{15}$$

where λ is an infrared regulator, and $I_\eta = 1$ in the K prescription. The phase is exactly compensated by an equal and opposite phase from FSI of line p_2. This irrelevant change of phase can be understood by the fact that the different prescriptions are related by a residual gauge transformation proportional to $\delta(k^+)$ which leaves the light-cone gauge $A^+ = 0$ condition unaffected.

Diffractive contributions which leave the target intact thus contribute at leading twist to deep inelastic scattering. These contributions do not resolve the quark structure of the target, and thus they are contributions to structure functions which are not parton probabilities. More generally, the rescattering contributions shadow and modify the observed inelastic contributions to DIS.

Our analysis in light-cone gauge resembles the "covariant parton model" of Landshoff, Polkinghorne and Short [97, 98] when interpreted in the target rest frame. In this description of small x DIS, the virtual photon with positive q^+ first splits into the pair p_1 and p_2. The aligned quark p_1 has no final state interactions. However, the antiquark line p_2 can interact in the target with an effective energy $\widehat{s} \propto k_{\mathrm{T}}^2/x$ while staying close to mass shell. Thus at small x and large $\widehat{s}$, the antiquark p_2 line can first multiply scatter in the target via pomeron and Reggeon exchange, and then it can finally scatter inelastically or be annihilated. The DIS cross section can thus be written as an integral of the $\sigma_{\overline{q}\mathrm{p}\to\mathrm{X}}$ cross section over the p_2 virtuality. In this way, the shadowing of the antiquark in the nucleus $\sigma_{\overline{q}\mathrm{A}\to\mathrm{X}}$ cross section yields the nuclear shadowing of DIS [93]. Our analysis, when interpreted in frames with $q^+ > 0$, also supports the color dipole description of deep inelastic lepton scattering at small x. Even in the case of the aligned jet configurations, one can understand DIS as due to the coherent color gauge interactions of the incoming quark-pair state of the photon interacting first coherently and finally incoherently in the target. For further discussion see Refs. [99] and [100]. The same final-state interactions, which produce leading-twist diffraction and shadowing in DIS, also lead to Bjorken-scaling single-spin asymmetries in semi-inclusive deep inelastic, see Refs. [29], [33] and [101].

This analysis has important implications for the interpretation of the nuclear structure functions measured in deep inelastic lepton scattering. Since leading-twist nuclear shadowing is due to the destructive interference of diffractive processes arising from final-state interactions (in the $q^+ \leq 0$ frame), the physics of shadowing is not contained in the wave functions of the isolated target alone. For example,

the light-front wave functions of stable states computed in light-cone gauge (PV prescription) are real, and they only sum the interactions within the bound-state which occur up to the light-front time $\tau = 0$ when the current interacts. Thus the shadowing of nuclear structure functions is due to the mutual interactions of the virtual photon and the target, not the nucleus in isolation [28].

6. Single-spin asymmetries from final-state interactions

Spin correlations provide a remarkably sensitive window to hadronic structure and basic mechanisms in QCD. Among the most interesting polarization effects are single-spin azimuthal asymmetries (SSAs) in semi-inclusive deep inelastic scattering, representing the correlation of the spin of the proton target and the virtual photon to hadron production plane: $\boldsymbol{S}_{\rm p} \cdot \boldsymbol{q} \times \boldsymbol{p}_{\rm H}$ [102]. Such asymmetries are time-reversal odd, but they can arise in QCD through phase differences in different spin amplitudes.

The most common explanation of the pion electroproduction asymmetries in semi-inclusive deep inelastic scattering is that they are related to the transversity distribution of the quarks in the hadron $\rm h_1$ [103 – 105] convoluted with the transverse momentum dependent fragmentation function $H_1^\perp$, the Collins function, which gives the distribution for a transversely polarized quark to fragment into an unpolarized hadron with non-zero transverse momentum [106 – 110].

Recently, an alternative physical mechanism for the azimuthal asymmetries has been proposed [29, 111, 112]. It was shown that the QCD final-state interactions (gluon exchange) between the struck quark and the proton spectators in semi-inclusive deep inelastic lepton scattering can produce single-spin asymmetries which survive in the Bjorken limit. In this case, the fragmentation of the quark into hadrons is not necessary, and one has a correlation with the production plane of the quark jet itself $\boldsymbol{S}_{\rm p} \cdot \boldsymbol{q} \times \boldsymbol{p}_q$. This final-state interaction mechanism provides a physical explanation within QCD of single-spin asymmetries. The required matrix element measures the spin-orbit correlation $\boldsymbol{S} \cdot \boldsymbol{L}$ within the target hadron's wave function, the same matrix element which produces the anomalous magnetic moment of the proton, the Pauli form factor, and the generalized parton distribution E which is measured in deeply virtual Compton scattering. Physically, the final-state interaction phase arises as the infrared-finite difference of QCD Coulomb phases for hadron wave functions with differing orbital angular momentum. The final-state interaction effects can be identified with the gauge link which is present in the gauge-invariant definition of parton distributions [111]. When the light-cone gauge is chosen, a transverse gauge link is required. Thus in any gauge the parton amplitudes need to be augmented by an additional eikonal factor incorporating the final-state interaction and its phase [112, 32]. The net effect is that it is possible to define transverse momentum dependent parton distribution functions which contain the effect of the QCD final-state interactions. The same final-state interactions are responsible for the diffractive component to deep inelastic scattering, and that they play a critical role in nuclear shadowing phenomena [28].

A related analysis also predicts that the initial-state interactions from gluon exchange between the incoming quark and the target spectator system lead to leading-twist single-spin asymmetries in the Drell-Yan process $\mathrm{H}_1\mathrm{H}_2^{\uparrow} \to \ell^+\ell^-\mathrm{X}$ [33, 113]. Initial-state interactions also lead to a $\cos 2\phi$ planar correlation in unpolarized Drell-Yan reactions [114].

The single-spin asymmetry (SSA) in semi-inclusive deep inelastic scattering (SIDIS) $\mathrm{ep}^{\uparrow} \to \mathrm{e}'\pi\mathrm{X}$, is given by the correlation $\boldsymbol{S}_{\mathrm{p}} \cdot \boldsymbol{q} \times \boldsymbol{p}_{\pi}$. For the electromagnetic interaction, there are two mechanisms for this SSA: $h_1 H_1^{\perp}$ and $f_{1T}^{\perp} D_1$. The former was first studied by Collins [106], and the latter by Sivers [115]. Hwang, Schmidt and and Brodsky have calculated [29] the single-spin Sivers asymmetry in semi-inclusive electroproduction $\gamma^*\mathrm{p}^{\uparrow} \to \mathrm{HX}$ induced by final-state interactions in a model of a spin-$\frac{1}{2}$ proton of mass M with charged spin-$\frac{1}{2}$ and spin-0 constituents of mass m and λ, respectively, as in the QCD-motivated quark-diquark model of a nucleon. The basic electroproduction reaction is then $\gamma^*\mathrm{p} \to q(qq)_0$. In fact, the asymmetry comes from the interference of two amplitudes which have different proton spin but couple to the same final quark spin state, and therefore it involves the interference of tree and one-loop diagrams with a final-state interaction. In this simple model the azimuthal target single-spin asymmetry $A_{\mathrm{UT}}^{\sin\phi}$ is given by

$$\begin{aligned} A_{\mathrm{UT}}^{\sin\phi} &= C_F \alpha_s(\mu^2)\, \frac{\Big(\Delta\, M + m\Big)\, r_\perp}{\Big[\, \Big(\, \Delta M + m\, \Big)^2 + \boldsymbol{r}_\perp^2\, \Big]} \\ &\times \left[\, \boldsymbol{r}_\perp^2 + \Delta(1-\Delta)\left(-M^2 + \frac{m^2}{\Delta} + \frac{\lambda^2}{1-\Delta}\right)\, \right] \\ &\times \frac{1}{\boldsymbol{r}_\perp^2}\, \ln \frac{\boldsymbol{r}_\perp^2 + \Delta(1-\Delta)\Big[-M^2 + m^2/\Delta + \lambda^2/(1-\Delta)\Big]}{\Delta(1-\Delta)\Big[-M^2 + m^2/\Delta + \lambda^2/(1-\Delta)\Big]}\,. \end{aligned} \tag{16}$$

Here $r_\perp$ is the magnitude of the transverse momentum of the current quark jet relative to the virtual photon direction, and $\Delta = x_{\mathrm{B}j}$ is the usual Bjorken variable. To obtain (16) from Eq. (21) of [29], we used the correspondence $\frac{|e_1 e_2|}{4\pi} \to C_F \alpha_s(\mu^2)$ and the fact that the sign of the charges e_1 and e_2 of the quark and diquark are opposite since they constitute a bound state. The result can be tested in jet production using an observable such as thrust to define the momentum $q + r$ of the struck quark.

The predictions of our model for the asymmetry $A_{\mathrm{UT}}^{\sin\phi}$ of the $\boldsymbol{S}_{\mathrm{p}} \cdot \boldsymbol{q} \times \boldsymbol{p}_q$ correlation based on Eq. (16) are shown in Fig. 7. As representative parameters we take $\alpha_s = 0.3$, $M = 0.94$ GeV for the proton mass, $m = 0.3$ GeV for the fermion constituent and $\lambda = 0.8$ GeV for the spin-0 spectator. The single-spin asymmetry $A_{\mathrm{UT}}^{\sin\phi}$ is shown as a function of Δ and $r_\perp$ (GeV). The asymmetry measured at HERMES [116] $A_{\mathrm{UL}}^{\sin\phi} = K A_{\mathrm{UT}}^{\sin\phi}$ contains a kinematic fac-

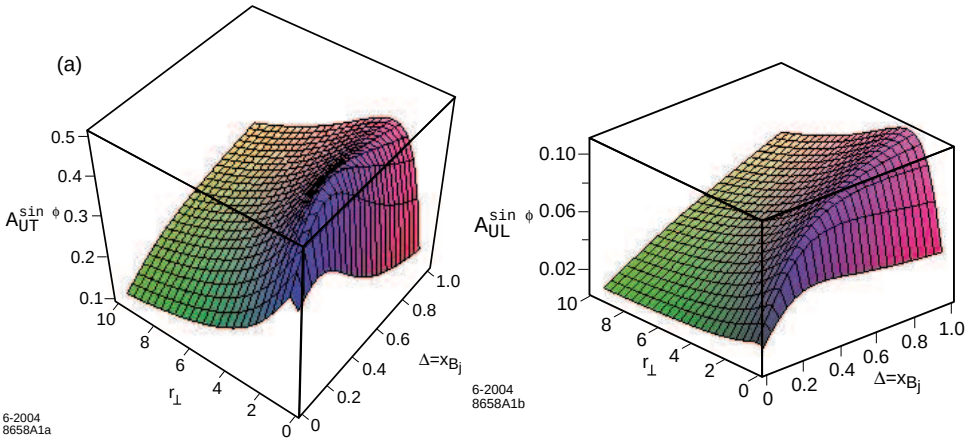

Fig. 7. Model predictions for the target single-spin asymmetry $A_{UT}^{\sin\phi}$ for charged and neutral current deep inelastic scattering resulting from gluon exchange in the final state. Here $r_\perp$ is the magnitude of the transverse momentum of the outgoing quark relative to the photon or vector boson direction, and $\Delta = x_{bj}$ is the light-cone momentum fraction of the struck quark. The parameters of the model are given in the text. In (a) the target polarization is transverse to the incident lepton direction. The asymmetry in (b) $A_{UL}^{\sin\phi} = K A_{UT}^{\sin\phi}$ includes a kinematic factor $K = \frac{Q}{\nu}\sqrt{1-y}$ for the case where the target nucleon is polarized along the incident lepton direction. For illustration, we have taken $K = 0.26\sqrt{x}$, corresponding to the kinematics of the HERMES experiment [116] with $E_{lab} = 27.6$ GeV and $y = 0.5$.

tor $K = (Q/\nu)\sqrt{1-y} = \sqrt{2Mx/E}\,\sqrt{(1-y)/y}$ because the proton is polarized along the incident electron direction. The resulting prediction for $A_{UL}^{\sin\phi}$ is shown in Fig. 7b. Note that $\boldsymbol{r} = \boldsymbol{p}_q - \boldsymbol{q}$ is the momentum of the current quark jet relative to the photon momentum. The asymmetry as a function of the pion momentum $\boldsymbol{p}_\pi$ requires a convolution with the quark fragmentation function.

Since the same matrix element controls the Pauli form factor, the contribution of each quark current to the SSA is proportional to the contribution $\kappa_{q/p}$ of that quark to the proton target's anomalous magnetic moment $\kappa_p = \sum_q e_q \kappa_{q/p}$ [29]. Avakian [102] has shown that the data from HERMES and Jefferson Lab could be accounted for by the above analysis. However, more analysis and measurements, especially azimuthal angular correlations, will be needed to unambiguously separate the transversity and Sivers effect mechanisms. Note that the Sivers effect occurs even for jet production; unlike transversity, hadronization is not required. There is no Sivers effect in charged current reactions since the W only couples to left-handed quarks [117].

The corresponding single spin asymmetry of the Drell-Yan processes, such as $\pi p^\uparrow$ (or $pp^\uparrow$) $\to \gamma^* X \to \ell^+\ell^- X$, is due to initial-state interactions. The simplest way to get the result is applying crossing symmetry to the SIDIS processes. The result that the SSA in the Drell-Yan process is the same as that obtained in SIDIS, with

the appropriate identification of variables, but with the opposite sign [111, 113].

We can also consider the SSA of e^+e^- annihilation processes such as $e^+e^- \to \gamma^* \to \pi\Lambda^\Uparrow X$. The Λ reveals its polarization via its decay $\Lambda \to p\pi^-$. The spin of the Λ is normal to the decay plane. Thus we can look for a SSA through the T-odd correlation $\epsilon_{\mu\nu\rho\sigma} S^\mu_\Lambda p^\nu_\Lambda q^\rho_{\gamma^*} p^\sigma_\pi$. This is related by crossing to SIDIS on a Λ target.

Measurements from Jefferson Lab [118] also show significant beam single spin asymmetries in deep inelastic scattering. Afanasev and Carlson [119] have recently shown that this asymmetry is due to the interference of longitudinal and transverse photoabsorption amplitudes which have different phases induced by the final-state interaction between the struck quark and the target spectators just as in the calculations of Ref. [29]. Their results are consistent with the experimentally observed magnitude of this effect. Thus similar FSI mechanisms involving quark orbital angular momentum appear to be responsible for both target and beam single-spin asymmetries.

Acknowledgements

I wish to thank Professor Ivan Supek and his colleagues at the Rudjer Boskovic Institute for hosting an outstanding nuclear and particle physics meeting at Dubrovnik. I also thank my collaborators, Carl Carlson, Guy de Teramond, Fred Goldhaber, Paul Hoyer, Dae Sung Hwang, Volodya Karmanov, Jungil Lee, Nils Marchal, Sven Menke, Carlos Merino, Gary McCartor, Stephane Peigne, Johan Rathsman, Francesco Sannino, and Ivan Schmidt, for their crucial input. This work was supported by the U.S. Department of Energy, contract DE–AC03–76SF00515.

References

[1] L. von Smekal, R. Alkofer and A. Hauck, Phys. Rev. Lett. **79** (1997) 3591 [arXiv:hep-ph/9705242].

[2] D. Zwanziger, Phys. Rev. D **69** (2002) 016002 [arXiv:hep-ph/0303028].

[3] D. M. Howe and C. J. Maxwell, Phys. Lett. B **541** (2002) 129 [arXiv:hep-ph/0204036].

[4] D. M. Howe and C. J. Maxwell, arXiv:hep-ph/0303163.

[5] A. C. Mattingly and P. M. Stevenson, Phys. Rev. D **49** (1994) 437 [arXiv:hep-ph/9307266].

[6] S. J. Brodsky, S. Menke, C. Merino and J. Rathsman, Phys. Rev. D **67** (2003) 055008 [arXiv:hep-ph/0212078].

[7] M. Baldicchi and G. M. Prosperi, Phys. Rev. D **66** (2002) 074008 [arXiv:hep-ph/0202172].

[8] S. J. Brodsky and H. J. Lu, Phys. Rev. D **51** (1995) 3652 [arXiv:hep-ph/9405218].

[9] S. J. Brodsky, E. Gardi, G. Grunberg and J. Rathsman, Phys. Rev. D **63** (2001) 094017 [arXiv:hep-ph/0002065].

[10] S. J. Brodsky, G. T. Gabadadze, A. L. Kataev and H. J. Lu, Phys. Lett. B **372** (1996) 133 [arXiv:hep-ph/9512367].

[11] S. J. Brodsky, G. P. Lepage and P. B. Mackenzie, Phys. Rev. D **28** (1983) 228.

[12] S. J. Brodsky, Y. Frishman and G. P. Lepage, Phys. Lett. B **167** (1986) 347.

[13] S. J. Brodsky, P. Damgaard, Y. Frishman and G. P. Lepage, Phys. Rev. D **33** (1986) 1881.

[14] V. M. Braun, S. E. Derkachov, G. P. Korchemsky and A. N. Manashov, Nucl. Phys. B **553** (1999) 355 [arXiv:hep-ph/9902375].

[15] J. Polchinski and M. J. Strassler, Phys. Rev. Lett. **88** (2002) 031601 [arXiv:hep-th/0109174].

[16] J. M. Maldacena, Adv. Theor. Math. Phys. **2**, 231 (1998) [Int. J. Theor. Phys. **38**, 1113 (1999)] [arXiv:hep-th/9711200].

[17] S. J. Brodsky and G. R. Farrar, Phys. Rev. Lett. **31** (1973) 1153.

[18] V. A. Matveev, R. M. Muradian and A. N. Tavkhelidze, Lett. Nuovo Cim. **7** (1973) 719.

[19] S. J. Brodsky and G. R. Farrar, Phys. Rev. D **11** (1975) 1309.

[20] S. J. Brodsky, M. Burkardt and I. Schmidt, Nucl. Phys. B **441** (1995) 197 [arXiv:hep-ph/9401328].

[21] S. J. Brodsky, H. C. Pauli and S. S. Pinsky, Phys. Rept. **301** (1998) 299 [arXiv:hep-ph/9705477].

[22] S. J. Brodsky and G. de Teramond, SLAC-PUB 10020 (2003) (in preparation).

[23] E. Tomboulis, Phys. Rev. D **8** (1973) 2736.

[24] P. P. Srivastava and S. J. Brodsky, Phys. Rev. D **64** (2001) 045006 [arXiv:hep-ph/0011372].

[25] S. J. Brodsky and D. S. Hwang, Nucl. Phys. B **543** (1999) 239 [arXiv:hep-ph/9806358].

[26] S. J. Brodsky, M. Diehl and D. S. Hwang, Nucl. Phys. B **596** (2001) 99 [arXiv:hep-ph/0009254].

[27] M. Diehl, T. Feldmann, R. Jakob and P. Kroll, Nucl. Phys. B **596** (2001) 33 [Erratum-ibid. **605** (2001) 647] [arXiv:hep-ph/0009255].

[28] S. J. Brodsky, P. Hoyer, N. Marchal, S. Peigne and F. Sannino, Phys. Rev. D **65** (2002) 114025 [arXiv:hep-ph/0104291].

[29] S. J. Brodsky, D. S. Hwang and I. Schmidt, Phys. Lett. B **530** (2002) 99 [arXiv:hep-ph/0201296].

[30] S. J. Brodsky and H. J. Lu, Phys. Rev. Lett. **64** (1990) 1342.

[31] S. Brodsky, P. Hoyer, G. Ingelman and R. Enberg, in progess.

[32] A. V. Belitsky, X. Ji and F. Yuan, Nucl. Phys. B **656** (2003) 165 [arXiv:hep-ph/0208038].

[33] J. C. Collins, Phys. Lett. B **536** (2002) 43 [arXiv:hep-ph/0204004].

[34] G. Grunberg, Phys. Lett. B **95** (1980) 70 [Erratum-ibid. **110** (1982) 501].

[35] G. Grunberg, Phys. Rev. D **29** (1984) 2315.

[36] S. J. Brodsky, M. S. Gill, M. Melles and J. Rathsman, Phys. Rev. D **58** (1998) 116006 [arXiv:hep-ph/9801330].

[37] S. J. Brodsky, M. Melles and J. Rathsman, Phys. Rev. D **60** (1999) 096006 [arXiv:hep-ph/9906324].

[38] K. Ackerstaff et al. [OPAL Collaboration], Eur. Phys. J. C **7** (1999) 571 [arXiv:hep-ex/9808019].

[39] F. Le Diberder and A. Pich, Phys. Lett. **B289** (1992) 165.

[40] M. Beneke and V. M. Braun, Phys. Lett. **B348** (1995) 513 [arXiv:hep-ph/9411229].

[41] P. Ball, M. Beneke and V. M. Braun, Nucl. Phys. B **452** (1995) 563 [arXiv:hep-ph/9502300].

[42] Y. L. Dokshitzer, G. Marchesini and B. R. Webber, Nucl. Phys. B **469** (1996) 93 [arXiv:hep-ph/9512336].

[43] S. J. Brodsky, C. R. Ji, A. Pang and D. G. Robertson, Phys. Rev. D **57** (1998) 245 [arXiv:hep-ph/9705221].

[44] B. Melić, B. Nižić and K. Passek, Phys. Rev. D **65** (2002) 053020 [arXiv:hep-ph/0107295].

[45] G. P. Lepage and S. J. Brodsky, Phys. Rev. D **22** (1980) 2157.

[46] R. C. Brower and C. I. Tan, Nucl. Phys. B **662** (2003) 393 [arXiv:hep-th/0207144].

[47] O. Andreev, Phys. Rev. D **67** (2003) 046001 [arXiv:hep-th/0209256].

[48] S. J. Brodsky, arXiv:hep-ph/0208158.

[49] S. J. Rey and J. T. Yee, Eur. Phys. J. C **22** (2001) 379 [arXiv:hep-th/9803001].

[50] G. 't Hooft, Nucl. Phys. B **72** (1974) 461.

[51] P. H. Frampton, Phys. Lett B **567** (2003) 265 [arXiv:hep-th/0305160].

[52] J. F. Gunion, S. J. Brodsky and R. Blankenbecler, Phys. Rev. D **8** (1973) 287.

[53] D. W. Sivers, S. J. Brodsky and R. Blankenbecler, Phys. Rept. **23** (1976) 1.

[54] R. Blankenbecler, S. J. Brodsky, J. F. Gunion and R. Savit, Phys. Rev. D **8** (1973) 4117.

[55] P. V. Landshoff, Phys. Rev. D **10** (1974) 1024.

[56] A. Duncan and A. H. Mueller, Phys. Lett. B **90** (1980) 159.

[57] S. J. Brodsky and G. P. Lepage, Phys. Rev. D **24** (1981) 2848.

[58] X. Ji, F. Yuan and J. P. Ma, Phys. Rev. Lett. **90** (2003) 241601.

[59] S. J. Brodsky, J. Hiller, D. S. Hwang and V. Karmanov (in preparation).

[60] A. V. Belitsky, X. Ji and F. Yuan, Phys. Rev. Lett. **91** (2003) 092003 [arXiv:hep-ph/0212351].

[61] J. Carbonell, B. Desplanques, V. A. Karmanov and J. F. Mathiot, Phys. Rep. **300** (1998) 215 [arXiv:nucl-th/9804029].

[62] S. Dalley, Nucl. Phys. B (Proc. Suppl.) **108** (2002) 145.

[63] R. L. Jaffe and A. Manohar, Nucl. Phys. B **337** (1990) 509.

[64] X. Ji, arXiv:hep-lat/0211016.

[65] S. J. Brodsky and S. D. Drell, Phys. Rev. D **22** (1980) 2236.

[66] S. J. Brodsky, arXiv:hep-th/0304106.

[67] S. J. Brodsky and A. H. Mueller, Phys. Lett. B **206** (1988) 685.

[68] G. Bertsch, S. J. Brodsky, A. S. Goldhaber and J. F. Gunion, Phys. Rev. Lett. **47** (1981) 297.

[69] L. Frankfurt, G. A. Miller and M. Strikman, Found. Phys. **30** (2000) 533 [arXiv:hep-ph/9907214].

[70] N. N. Nikolaev, W. Schafer and G. Schwiete, Phys. Rev. D **63** (2001) 014020 [arXiv:hep-ph/0009038].

[71] E. M. Aitala et al. [E791 Collaboration], Phys. Rev. Lett. **86** (2001) 4773 [arXiv:hep-ex/0010044].

[72] E. M. Aitala et al. [E791 Collaboration], Phys. Rev. Lett. **86** (2001) 4768 [arXiv:hep-ex/0010043].

[73] J. Gronberg et al. [CLEO Collaboration], Phys. Rev. D **57** (1998) 33 [arXiv:hep-ex/9707031].

[74] G. P. Lepage and S. J. Brodsky, Phys. Lett. B **87** (1979) 359.

[75] A. V. Efremov and A. V. Radyushkin, Theor. Math. Phys. **42** (1980) 97 [Teor. Mat. Fiz. **42** (1980)147].

[76] V. A. Karmanov and A.V. Smirnov, Nucl. Phys. A **546** (1992) 691.

[77] M. K. Jones et al. [Jefferson Lab Hall A Collaboration], Phys. Rev. Lett. **84** (2000) 1398 [arXiv:nucl-ex/9910005].

[78] O. Gayou et al. [Jefferson Lab Hall A Collaboration], Phys. Rev. Lett. **88** (2002) 092301 [arXiv:nucl-ex/0111010].

[79] B. V. Geshkenbein, B. .L. Ioffe and M. A. Shifman, Sov. J. Nucl. Phys. **20** (1975) 66 [Yad. Fiz. **20** (1974) 128].

[80] S. J. Brodsky, C. E. Carlson, J. Hiller and D. S. Hwang in preparation.

[81] G. Duplančić and B. Nizić, arXiv:hep-ph/0304255.

[82] M. Beneke, G. Buchalla, M. Neubert and C. T. Sachrajda, Nucl. Phys. B **591** (2000) 313 [arXiv:hep-ph/0006124].

[83] Y. Y. Keum, H. N. Li and A. I. Sanda, Phys. Rev. D **63** (2001) 054008 [arXiv:hep-ph/0004173].

[84] A. Szczepaniak, E. M. Henley and S. J. Brodsky, Phys. Lett. B **243** (1990) 287.

[85] S. J. Brodsky, arXiv:hep-ph/0104153.

[86] C. K. Chua, W. S. Hou and S. Y. Tsai, Phys. Rev. D **66** (2002) 054004 [arXiv:hep-ph/0204185].

[87] S. J. Brodsky, A. S. Goldhaber and J. Lee, arXiv:hep-ph/0305269.

[88] K. Abe et al. [Belle Collaboration], Phys. Rev. Lett. **89** (2002) 142001 [arXiv:hep-ex/0205104].

[89] J. C. Collins, arXiv:hep-ph/0304122.

[90] L. Stodolsky, Phys. Rev. Lett. **18** (1967) 135.

[91] V. N. Gribov, Sov. Phys. JETP **29** (1969) 483 [Zh. Eksp. Teor. Fiz. **56** (1969) 892].

[92] S. J. Brodsky and J. Pumplin, Phys. Rev. **182** (1969) 1794.

[93] S. J. Brodsky and H. J. Lu, Phys. Rev. Lett. **64** (1990) 1342.

[94] G. Piller and W. Weise, Phys. Rept. **330** (2000) 1 [arXiv:hep-ph/9908230].

[95] Y. V. Kovchegov, Phys. Rev. D **55** (1997) 5445 [arXiv:hep-ph/9701229].

[96] G. Leibbrandt, Rev. Mod. Phys. **59** (1987) 1067.

[97] P. V. Landshoff, J. C. Polkinghorne and R. D. Short, Nucl. Phys. B **28** (1971) 225.

[98] S. J. Brodsky, F. E. Close and J. F. Gunion, Phys. Rev. D **8** (1973) 3678.

[99] S. J. Brodsky, arXiv:hep-ph/0109205.

[100] P. Hoyer, arXiv:hep-ph/0209317.

[101] A. V. Efremov, K. Goeke and P. Schweitzer, Phys. Lett B **568** (2003) 63 [arXiv:hep-ph/0303062].

[102] H. Avakian [CLAS Collaboration], *Workshop on Testing QCD through Spin Observables in Nuclear Targets*, Charlottesville, Virginia, 18-20 Apr 2002

[103] R.L. Jaffe, hep-ph/9602236.

[104] D. Boer, Nucl. Phys. Proc. Suppl. **105** (2002) 76 [hep-ph/0109221].

[105] D. Boer, Nucl. Phys. A **711** (2002) 21 [hep-ph/0206235].

[106] J.C. Collins, Nucl. Phys. **B 396** (1993) 161.

[107] V. Barone, A. Drago and P.G. Ratcliffe, Phys. Rept. **359** (2002) 1.

[108] B. Q. Ma, I. Schmidt and J. J. Yang, Phys. Rev. D **66** (2002) 094001 [arXiv:hep-ph/0209114].

[109] G. R. Goldstein and L. Gamberg, arXiv:hep-ph/0209085.

[110] L. P. Gamberg, G. R. Goldstein and K. A. Oganessyan, Phys. Rev. D **67** (2003) 071504 [arXiv:hep-ph/0301018].

[111] J.C. Collins, Phys. Lett. B **536** (2002) 43.

[112] X. Ji and F. Yuan, Phys. Lett. B **543** (2002) 66.

[113] S. J. Brodsky, D. S. Hwang and I. Schmidt, Nucl. Phys. B **642** (2002) 344.

[114] D. Boer, S. J. Brodsky and D. S. Hwang, Phys. Rev. D **67** (2003) 054003 [arXiv:hep-ph/0211110].

[115] D. W. Sivers, Phys. Rev. D **43** (1991) 261.

[116] A. Airapetian et al. [HERMES Collaboration], Phys. Rev. Lett. **84** (2000) 4047.

[117] S. J. Brodsky, D. S. Hwang and I. Schmidt, Phys. Lett. B **553** (2003) 223 [arXiv:hep-ph/0211212].

[118] H. Avakian et al. [CLAS Collaboration], [arXiv:hep-ex/0301005].

[119] A. Afanasev and C. E. Carlson, [arXiv:hep-ph/0308163].

NOVI IZGLEDI ZA QCD: GOTOVO-KONFORMNI QCD I NOVI UČINCI MEĐUDJELOVANJA U KONAČNOM STANJU

Efektivan naboj QCD, izveden iz raspada tauona, iznenađujuće je stalan pri malim impulsima, što ukazuje na gotovo-konformna svojstva hadronskih međudjelovanja pri malim prijenosima impulsa. Odnos supergravitacijske teorije u višedimenzijskim anti-de Sitterovim prostorima za velike N_C s baždarnom teorijom u fizičkom prostoru-vremenu, također daje zanimljive zaključke o hadronskoj fenomenologiji u konformnoj granici, kao što su pravila za brojanje sastavnica (konstituenata) u tvrdim ekskluzivnim procesima. Daje se pregled korisnosti kvantizacije i Fockovih valnih funkcija na svjetlosnoj fronti u analizama takvih pojava i za predstavljanje dinamike vezanih stanja QCD. Raspravljamo nove učinke međudjelovanja u početnom i konačnom stanju u tvrdim ekskluzivnim procesima, uključujući jednospinske asimetrije u Bjorkenovom sumjerilu te difraktivne i zasjenjene doprinose vodećih tzv. "twist" članova duboko-neelastičnom raspršenju elektron-proton.